Cellular/Molecular

Calpains, Cleaved Mini-Dysferlin$_{C72}$, and L-Type Channels Underpin Calcium-Dependent Muscle Membrane Repair

Angela Lek,[1,2] Frances J. Evesson,[1,2] Frances A. Lemckert,[1,2] Gregory M. I. Redpath,[1,2] Ann-Katrin Lueders,[1] Lynne Turnbull,[3] Cynthia B. Whitchurch,[3] Kathryn N. North,[1,2] and Sandra T. Cooper[1,2]

[1]Institute for Neuroscience and Muscle Research, Children's Hospital at Westmead, Sydney, NSW 2145, Australia, [2]Discipline of Paediatrics and Child Health, Faculty of Medicine, University of Sydney, Sydney, NSW 2006, Australia, and [3]Microbial Imaging Facility, ithree institute, University of Technology Sydney, Broadway, NSW 2007, Australia

Dysferlin is proposed as a key mediator of calcium-dependent muscle membrane repair, although its precise role has remained elusive. Dysferlin interacts with a new membrane repair protein, mitsugumin 53 (MG53), an E3 ubiquitin ligase that shows rapid recruitment to injury sites. Using a novel ballistics assay in primary human myotubes, we show it is not full-length dysferlin recruited to sites of membrane injury but an injury-specific calpain-cleavage product, mini-dysferlin$_{C72}$. Mini-dysferlin$_{C72}$-rich vesicles are rapidly recruited to injury sites and fuse with plasma membrane compartments decorated by MG53 in a process coordinated by L-type calcium channels. Collective interplay between activated calpains, dysferlin, and L-type channels explains how muscle cells sense a membrane injury and mount a specialized response in the unique local environment of a membrane injury. Mini-dysferlin$_{C72}$ and MG53 form an intricate lattice that intensely labels exposed phospholipids of injury sites, then infiltrates and stabilizes the membrane lesion during repair. Our results extend functional parallels between ferlins and synaptotagmins. Whereas otoferlin exists as long and short splice isoforms, dysferlin is subject to enzymatic cleavage releasing a synaptotagmin-like fragment with a specialized protein- or phospholipid-binding role for muscle membrane repair.

Introduction

Skeletal muscle membrane repair became a topic of intense research interest when it was implicated in the pathogenesis of muscular dystrophy. Mutations in the dysferlin gene were identified as a new cause of muscular dystrophy (Bashir et al., 1998; Liu et al., 1998), and dysferlin-deficient mouse myofibers were shown to demonstrate defective calcium-dependent membrane repair (Bansal et al., 2003). Dysferlin is a member of the ferlin family of vesicle fusion proteins characterized by the rare feature of six or seven tandem C2 domains (Lek et al., 2012), motifs associated with calcium-regulated lipid or protein binding. Thus, dysferlin emerged as a key mediator of calcium-activated vesicle-mediated membrane repair. Pathologies relating to defective vesicle fusion link ferlin animal models (Washington and Ward, 2006; Covian-Nares et al., 2010), with mutations in human otoferlin causing a form of inherited human deafness resulting from defective synaptic vesicle fusion in the cochlea (Roux et al., 2006; Dulon et al., 2009; Johnson and Chapman, 2010).

Recently, it has been demonstrated that dysferlin interacts with a new membrane repair protein, mitsugumin 53 (MG53, also called TRIM72) (Cai et al., 2009b). MG53 bears the characteristic structural motifs of a TRIM-domain E3-ubiquitin ligase and rapidly accumulates at sites of membrane damage (Cai et al., 2009b). MG53 knock-out mice display a mild, progressive muscular dystrophy that is also characterized by defective membrane resealing of skeletal myofibers (Cai et al., 2009a). The substrate of the MG53 E3 ligase is unknown; however, MG53 is proposed to participate in calcium-independent stages of membrane resealing via formation of a disulphide-linked protein scaffold to which membrane repair components bind (Cai et al., 2009a), such as dysferlin.

Although it has long been established that damaged cells require calcium to survive a membrane injury (Steinhardt et al., 1994), molecular roles for calcium in the resealing response are unclear. There are three families of calcium-binding proteins with proposed roles in membrane repair: dysferlin (Bansal et al., 2003), annexins (McNeil et al., 2006; Bouter et al., 2011), and calpains (Mellgren et al., 2009). We developed a novel ballistics assay to study the acute responses of human skeletal myotubes to a membrane injury. Using rapid fixation, we "freeze-frame" injury repair, and have used confocal and super-resolution 3D-

Received July 25, 2012; revised Dec. 2, 2012; accepted Jan. 13, 2013.

Author contributions: A.L. and S.T.C. designed research; A.L., F.J.E., F.A.L., G.M.I.R., A-K.L., L.T., and S.T.C. performed research; A.L., C.B.W., and K.N.N. contributed unpublished reagents/analytic tools; A.L., A-K.L., L.T., and S.T.C. analyzed data; A.L. and S.T.C. wrote the paper.

This work was supported by the Australian National Health and Medical Research Council Project Grant 570744 to S.T.C. and K.N.N., Australian Postgraduate Award to A.L., Fellowship 571905 to C.B.W., the Jain Foundation (S.T.C.), the NSW Muscular Dystrophy Association (S.T.C., K.N.N.), and the Brain Foundation (S.T.C., K.N.N.). We thank Dr Neil Street (Department of Anaesthesia, Children's Hospital at Westmead) for his assistance with patient and control biopsy samples for primary culture; Dr. X. M. Wang in the Flow Cytometry Core Facility at Westmead Millennium Institute (supported by the Australian National Health and Medical Research Council and Cancer Institute New South Wales) for performing flow cytometry; Prof. Jianjie Ma and Dr. Noah Weisleder (UMNDJ, Piscataway, New Jersey) for the polyclonal anti-MG53 antibody; Bodson designs (Sydney, Australia) for the graphic design for Figure 7; and our patients and their families.

The authors declare no competing financial interests.

Correspondence should be addressed to Dr. Sandra T. Cooper, Institute for Neuroscience and Muscle Research, Children's Hospital at Westmead, Locked Bag 4001, Westmead, NSW 2145, Australia. E-mail: sandra.cooper@sydney.edu.au.

DOI:10.1523/JNEUROSCI.3560-12.2013

 0270-6474/13/335085-10$15.00/0

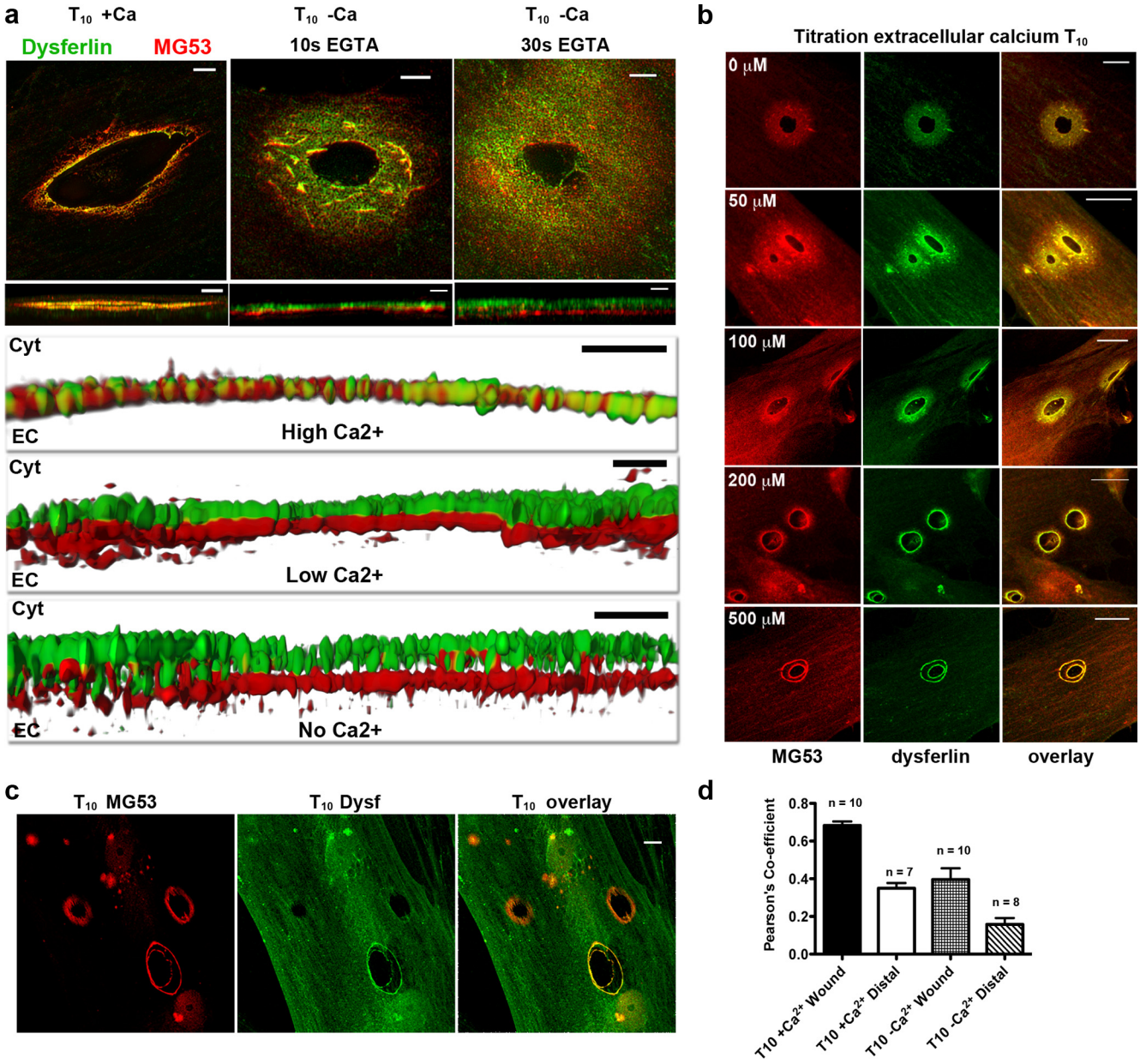

Figure 1. Dysferlin and MG53 show rapid, calcium-dependent accumulation at injury sites. ***a***, 3D-SIM. Left, Dysferlin (green) and MG53 (red) form a concentrated lattice encircling injury sites in "+Ca," interdigitating within the same *xz* plane (bottom rows). In low calcium conditions (middle: 10 s EGTA chelation, shot −Ca buffer) or −Ca conditions (right: 30 s EGTA chelation, shot −Ca buffer), dysferlin and MG53 remain as diffuse halos and occupy discrete spatial compartments in the *xz* plane (bottom rows), observed as clusters of dysferlin-rich vesicles positioned adjacent to plasma membrane compartments enriched with MG53. First row: scale bar, 2 μm. Zoomed images and *xz* slices: scale bar, 0.5 μm. ***b***, MG53 and dysferlin transition from a diffuse halo in −Ca/low calcium, into concentrated rings at injury sites with >200 μM extracellular calcium. Scale bars, 10 μm. ***c***, MG53 remains diffusely enriched at dysferlin-negative ballistics lesions. Scale bars, 4 μm. ***d***, In the presence of calcium, MG53 and dysferlin colocalize at the wound site; a Pearson coefficient (Costes et al., 2004) of ~0.7 is consistent with interdigitated and partially overlapping dysferlin and MG53 compartments. Distal to the wound site, or in the absence of calcium, dysferlin and MG53 do not colocalize (Pearson coefficient <0.4).

structured illumination microscopy (3D-SIM) to reconstruct the spatial and temporal assembly of endogenously expressed muscle membrane repair proteins. Our results unify discrete calcium-dependent roles for activated calpains and dysferlin that function upstream of recruited annexins. Moreover, we propose the calcium dependence of membrane repair involves unique interplay between cellular signaling pathways activated both by calcium entry via the membrane lesion, and by L-type voltage-gated calcium channels (VGCCs) in response to the persistent depolarization induced by a membrane breach. Together, these signaling pathways initiate a specialized response to membrane injury.

Materials and Methods

Primary myoblast culture

Human muscle biopsy samples were minced into 1–2 mm pieces and transferred into a scored, collagen-coated T25 with 1 ml of growth media containing 20% FCS, 10% amniomax, 1:200 gentamycin, 1:1 DMEM: Ham's F12 (Invitrogen). Flasks were sealed to retain humidity and supplemented with 2 ml fresh growth media after 48 h. Myoblast outgrowth was typically observed 48–72 h after plating. Expanded cultures were trypsinized, and myoblast-rich cultures derived through fluorescent cell sorting for anti-NCAM$^{PE\text{-}CY7}$ labeling (mouse anti-human CD56, BD Biosciences). Myoblasts were induced to differentiate by culture in dif-

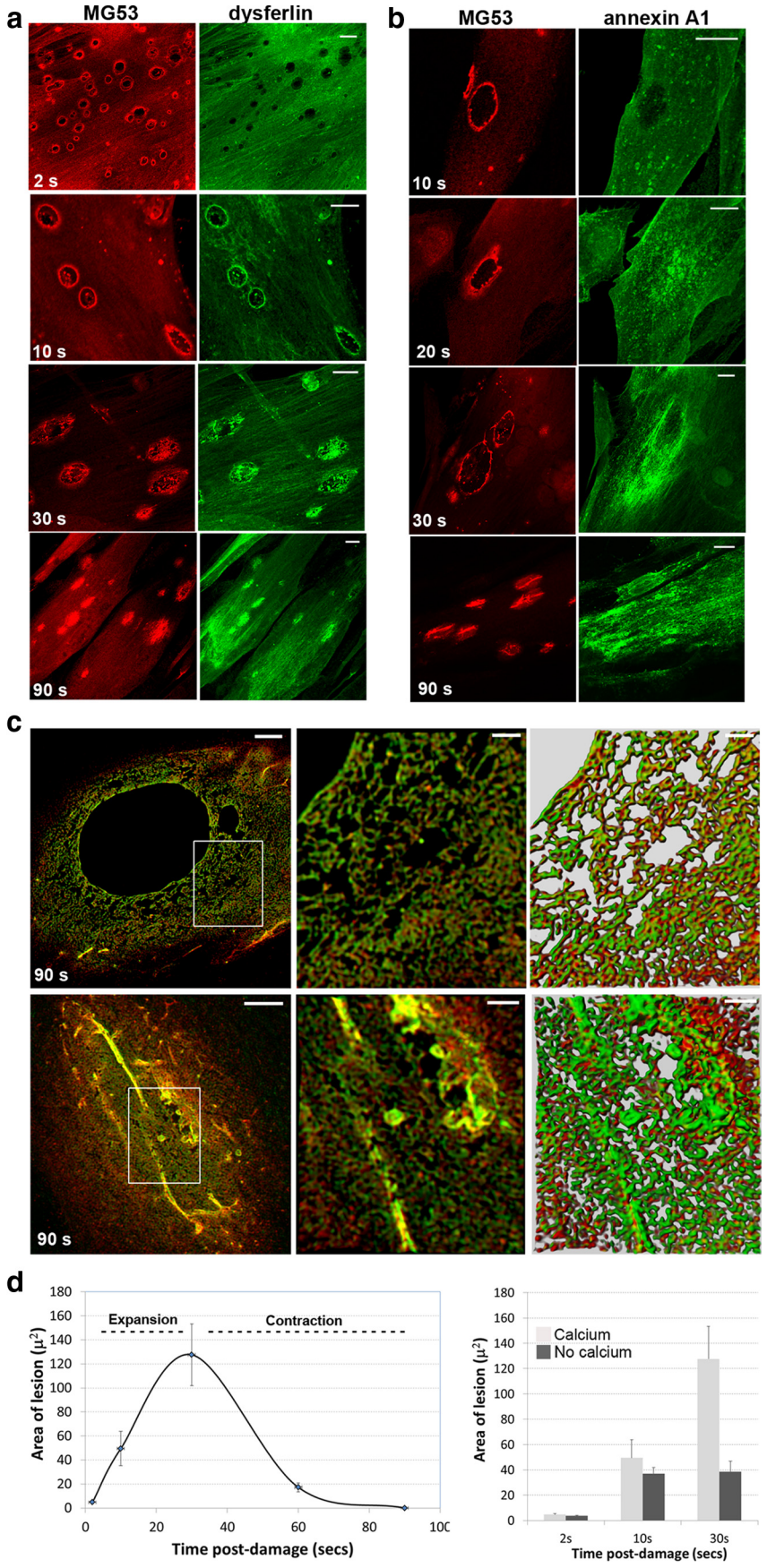

Figure 2. Temporal sequence of injury-activated recruitment of MG53, dysferlin, and annexin A1. Representative confocal images of MG53 and dysferlin (***a***) and MG53 and annexin A1 (***b***) recruitment to sites of injury in primary human myotubes fixed at 2, 10, 30, and 90 s after injury. Scale bar: 10 μm. ***c***, 3D-SIM of two lesions at 90 s after injury; an unfilled lesion (top) with an expansive dysferlin (green) and MG53 (red) lattice surrounding the injury site, and a filled lesion (bottom) with the characteristic arc of strongly labeled dysferlin and MG53 among a tightly woven lattice. ***d***, Ballistics lesions in human skeletal myotubes showed calcium-dependent expansion and contraction phases of membrane resealing. Points on the line graph (left) represent the average area (Leica SP2 ellipse formula) of lesions at 2 s ($n = 44$), 10 s ($n = 40$), 30 s ($n = 47$), and 60 s ($n = 40$); error bars indicate SE. The area at 90 s was set to 0 to reflect resealed patches. Histogram (right) shows the lack of expansion of ballistics lesions in −Ca conditions (2 s, $n = 45$; 10 s, $n = 44$; 30 s, $n = 45$). Later time points for −Ca conditions could not be calculated because of cellular lethality caused by injury in −Ca.

ferentiation media (1:1 DMEM:Ham's F12, 3% horse serum, 1:200 gentamycin) for 4–5 d.

Control myoblasts. Biopsies (male and female) subjected to malignant hypothermia testing with normal *in vitro* contracture results.

Patient myoblasts. Patient myoblasts were as follows: Dysferlinopathy 1 (female), L344P, and splice acceptor site preceding exon 49; Dysferlinopathy 2 and Dysferlinopathy 3 are male siblings, Q1061_A1062insAE and R1586X; sarcoglycanopathy homozygous R77C (male); caveolinopathy E33K (female). Ethical approval for this research project was provided by the Children's Hospital at Westmead (10/CHW/45).

Ballistics-induced membrane damage

Ballistics-induced injury was performed using a Bio-Rad Helios Gene Gun with bullet cartridges prepared using silica microparticles (4 μm diameter, Sigma). Myotubes on Thermanox coverslips and differentiated for 4–6 d were shot at 300 psi in a 24-well containing 200 μl PBS (Invitrogen) in a laminar flow hood. Immediately after discharging the gun, 200 μl PBS was immediately added to the well to refresh the fluid expelled by the helium blast.

Minus calcium conditions. Coverslips were preincubated in 500 μl calcium-free PBS containing 10 mM EGTA for 30 s, then shot in 200 μl calcium-free PBS.

Trypan permeability. To assess membrane permeability of shot myotubes, trypan blue was added to shot and unshot myotubes at 2, 10, 30, 60, and 120 s after injury. Shot myotubes were shown to exclude trypan blue at 120 s after injury in the presence of calcium, but not in calcium-free buffer, consistent with impaired resealing in −Ca conditions.

Calcium-titration. Calcium-free PBS was mixed at the appropriate ratio with calcium-containing PBS (0.9 μM). Addition of calcium chloride was used for concentrations >0.9 μM. All solutions used were equalized to room temperature (23°C–26°C).

Calcium-channel inhibitors. A total of 100 mM stocks of cadmium-, nickel-, and gadolinium-chloride (Sigma) were diluted in PBS to a final concentration of 800 μM. Stocks of diltiazem (50 mM in MQ), verapamil (50 mM in MQ), and nifedipine (50 mM in DMSO) were freshly prepared

and diluted in PBS just before the experiment. Differentiated human myotubes were preincubated with diltiazem (50 μM), nifedipine (100 μM), or verapamil (100 μM) for 1 h in culture media before injury, preincubated for 30 s in PBS containing the same inhibitor, then shot in PBS containing the inhibitor.

Immunocytochemistry

For the ballistics time course, the T_2 sec sample was obtained by flooding the shot well with 500 μl ice-cold fixative (3% PFA in PBS containing 20% sucrose, pH 7). For other time points, shot coverslips were picked up using a bent needle and forceps and transferred onto droplets of ice-cold fixative on a Parafilm-covered glass plate resting on ice. After fixation, coverslips were washed (3 dips in room temperature PBS baths), permeabilized with PBS plus 0.15% saponin for 10 min, washed, devitellinized with room temperature methanol/acetone 1:1 for 4 min, washed, blocked (PBS containing 2% BSA) for 30 min, then incubated in primary antibody diluted in block overnight in the cold room. Coverslips were washed, reblocked for 15 min, incubated with secondary antibody diluted in block for 2 h, washed and mounted on a 22 × 50 mm glass coverslips with a droplet of Fluorsave (Calbiochem) or Vectashield (Vector Laboratories) mounting reagents.

Antibodies

Western blot. Western blot included the following: Hamlet-1 (Novocastra, 1:500), Romeo-1 (Epitomics, 1:500), anti-sarcomeric actin 5C5 (Sigma, 1:1000), and anti-GAPDH (Millipore Bioscience Research Reagents, 1:2000).

Immunocytochemistry. Immunocytochemistry included the following: Hamlet-1 (1:25), Hamlet-2 (Novocastra, 1:25), Romeo-1 (1:200), SAB2100636 (Sigma, 1:200), MG53 rabbit polyclonal (gift from Prof. Jianjie Ma, 1:200), annexin A1 (BD Biosciences, 1:100), annexin A2 (BD Biosciences, 1:100), AHNAK (Sapphire Bioscience, 1:250), caveolin-3 (BD Biosciences, 1:500), syntaxin-4 (Synaptic Systems, 1:250), Munc-18 (Edwards Scientific, 1:250), dystrophin (Novocastra, NCL-DYS3, 1:50), annexin V (Sapphire Bioscience, 1:50), LAMP-1 (Hybridoma Bank, H4A3, 1:500), GM130 (BD Biosciences, 1:100), VAMP-4 (Synaptic Systems, 1:200), and goat anti-rabbit^{Alexa594}, goat anti-rabbit^{Alexa555}, and donkey anti-mouse^{Alexa488} (Invitrogen, 1:200).

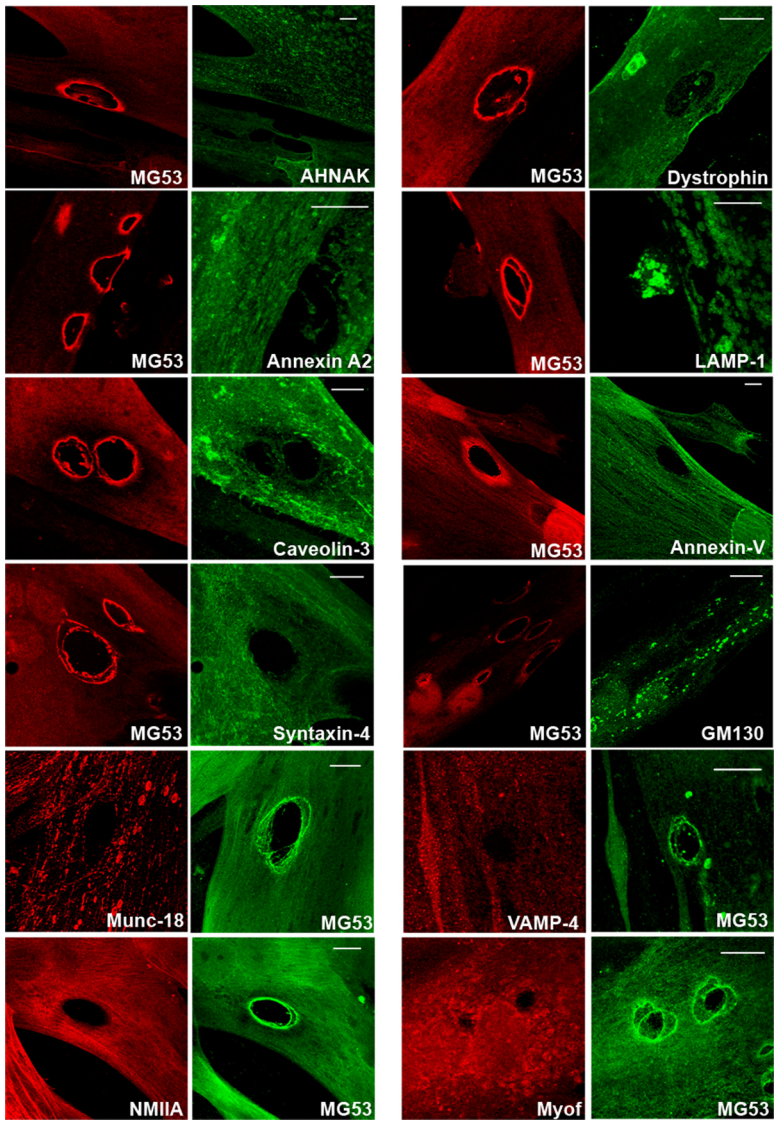

Figure 3. Screening for injury-activated recruitment of other muscular dystrophy proteins and endomembrane markers 10 s after ballistics injury of human skeletal myotubes. Rapid recruitment to injury sites is a specific feature of dysferlin and MG53, not observed for myoferlin, AHNAK, caveolin-3, or dystrophin. Moreover, we could find no evidence for specific recruitment of endomembrane compartments labeled for syntaxin-4, Munc-18c, VAMP-4, GM130, or annexin V, or molecular motor nonmuscle myosin 2A. Of note, we did not observe enrichment of LAMP-1 (or LAMP-2, data not shown) at sites of membrane injury in human myotubes, although we occasionally observed evidence for lysosomal exocytosis at sites distal to the membrane injury: the membrane bleb positively labeled for LAMP-1 directly adjacent to the site of membrane injury labeled by MG53.

Scrape injury and cell harvesting

Cells grown in 6-well plates were washed once with 2 ml ice-cold PBS containing freshly added protease inhibitor mixture (1:500, Sigma-Aldrich, P8340), then solubilized in 250 μl RIPA (50 mM Tris, pH 7.4, 150 mM NaCl, 1% Nonidet P-40, 0.5% deoxycholate, 0.1% SDS, 1 mM EDTA, 1:500 protease inhibitor mixture) for 30 min on ice with gentle rocking. Samples were collected and centrifuged for 1 min at 13,000 × *g* to pellet cell debris. Supernatant was transferred to a fresh tube and snap frozen at −80°C. Cells grown in 6-well plates were washed once with room temperature PBS (24°C-26°C), scraped with a rubber policeman in 500 μl PBS, and pelleted by centrifugation for 5 min at 300 × *g*. Supernatant was removed and cell pellets were resuspended in RIPA, rotated at 4°C for 30 min, then centrifuged for 1 min at 13,000 × *g* to pellet cell debris. Supernatant was transferred to a fresh tube and snap frozen at −80°C.

SDS-PAGE and Western blotting

RIPA supernatants were reconstituted to 1 × SDS loading buffer (1% SDS 5.5% glycerol, 55 mM DTT, bromophenol blue). A total of 10 μg total protein was separated on Nu-PAGE 4–12% gradient gels, transferred to PVDF membranes, and probed with antibodies diluted in block (PBS plus 0.1% Tween, 5% skim milk) as previously described (Waddell et al., 2011).

Microscopy

Confocal. Images were captures using a Leica SP2 or SP5 scanning confocal microscope with a 63× oil objective.

3D-SIM. Imaging was performed using a DeltaVision OMX V3 3D-Structured Illumination Microscopy System (OMX 3D-SIM, Applied Precision) as previously described (Riglar et al., 2011). Raw 3-phase images were reconstructed as previously described (Gustafsson et al., 2008; Schermelleh et al., 2008). Reconstructed images were rendered in 3D, with interpolation, using IMARIS v. 7.4 (Bitplane Scientific). Colocalization correlation was performed according to Costes et al. (2004), using

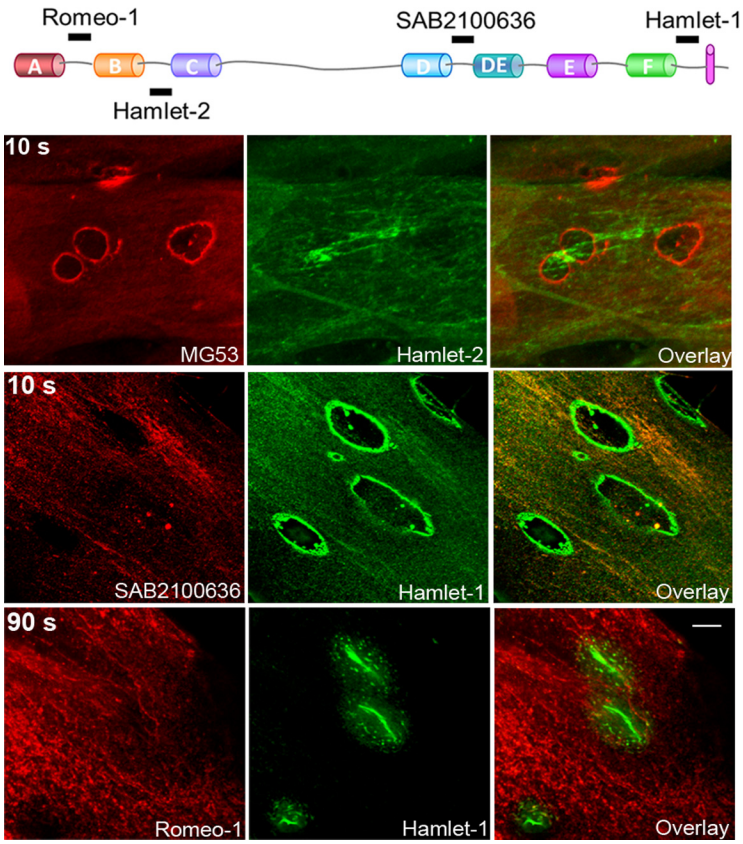

Figure 4. Injury-recruited dysferlin is only recognized by the C-terminal Hamlet-1 antibody. Dysferlin antibodies recognizing N-terminal epitopes do not detect dysferlin at injury sites at 10 s after injury (Hamlet-2, top row; anti-C2DE SAB2100636, middle row) or 90 s after injury (Romeo-1, bottom row).

IMARIS software. Correct alignment of the individual fluorescent channels was validated using Tetraspec beads (Invitrogen) before image capture.

Results

Our study exploited the advantage of rapid ballistics injury to resolve the acute response of human skeletal myotubes to membrane injury, with the specific goal of determining the interplay between the calcium-independent injury response proposed for MG53 (Cai et al., 2009a), with calcium-dependent elements of membrane repair proposed for dysferlin (Bansal et al., 2003). Using trypan blue exclusion as a marker of membrane permeability, we established ballistics conditions that created membrane lesions that were repairable within 2 min (data not shown, see Materials and Methods). Immunolabeling of coverslips damaged via ballistics at 10 s after injury reveals that both dysferlin and MG53 show rapid, calcium-dependent stages of injury recruitment (Fig. 1*a*, 10 s after injury). 3D-SIM reveals that, in the presence of physiological calcium, dysferlin and MG53 compartments interdigitate to form a concentrated lattice, specifically bound to exposed lipids encircling ballistics lesions (Fig. 1*a*, left, +Ca). When extracellular calcium is chelated by EGTA (30 s) and myotubes are shot in calcium-free buffer, dysferlin and MG53 still show enrichment to injury sites but appear as diffuse halos surrounding ballistics lesions (Fig. 1*a*, right). Moreover, rotation of −Ca lesions in the *x*-*z* plane reveals dysferlin and MG53 occupy distinct spatial planes, with dysferlin-rich vesicular compartments lying on the cytoplasmic face of accumulated MG53 on the plasma membrane (Fig. 1*a*, right, bottom rows). Using only brief chelation with EGTA (10 s vs 30 s), we captured intermediates of dysferlin and MG53 merging, with small rafts of aligned but unfused dysferlin-rich vesicles on the cytoplasmic face of MG53 clusters at the plasma membrane (Fig. 1*a*, middle). By titrating levels of extracellular calcium, we show that $\geq$200 μM $[Ca]_{EC}$ provides the critical calcium concentration required to activate fusion of dysferlin and MG53 compartments, and their refinement into a concentrated lattice specifically bound to the exposed lipids at the edge of injury sites (Fig. 1*b*).

We occasionally observed ballistics lesions positive for MG53 but negative for dysferlin (Fig. 1*c*). At these sites, MG53 labeling remained as a diffuse halo, similar to −Ca conditions. Furthermore, distal to injury sites, and in −Ca conditions, we observed little or no colocalization of dysferlin and MG53 (Fig. 1*a*,*d*; Pearson coefficient <0.4). Collectively, our results imply that MG53 and dysferlin have separate routes of injury-activated recruitment. Therefore, dysferlin is not required to trigger MG53 injury recruitment but is associated with a calcium-dependent phase of MG53 accumulation at injury sites.

We next studied the temporal sequence of injury-activated recruitment of MG53 and dysferlin, with that of annexin-A1, a phospholipid-binding protein also implicated in membrane repair (McNeil et al., 2006). We have previously shown that annexin-A1, together with dysferlin and MG53, colabel damaged longitudinal tubules in overstretched human muscle (Waddell et al., 2011). MG53 showed diffuse enrichment at injury sites at 2 s after injury (Fig. 2*a*), before robust detection of dysferlin. By 10 s after injury, MG53 and dysferlin intensely labeled the circumference of the ballistics lesions. In contrast, enrichment of vesicular compartments labeled by annexin-A1 only became evident at 20–30 s post-injury, but did not show specificity for the lesion site, instead showing amorphous labeling peripheral to the membrane lesions (Fig. 2*b*). The concentrated lattice formed by dysferlin and MG53 encircling injury sites at early time points expands and spreads throughout the injury site during repair (Fig. 2*a*, 30–90 s after injury). At 90 s after injury, lesions appear as "filled patches" that appear as a network of invaginating membranes (Fig. 2*a*, 90 s), often characterized by a dominant arc of labeled membrane (Fig. 2*b*, 90 s; see Fig. 4, 90 s). 3D-SIM of two lesions at 90 s after injury represent the two outcomes observed at this time point, an unfilled lesion with an expansive dysferlin and MG53 lattice surrounding the injury site (Fig. 2*c*, top), and a filled lesion with the characteristic arc of strongly labeled dysferlin and MG53 among a bed of interdigitated lattice (Fig. 2*c*, bottom).

Repair of ballistics injury in human skeletal myotubes showed calcium-dependent expansion and contraction phases of membrane resealing (Fig. 2*d*), as previously reported using an *in vivo* model of membrane injury within a developing Drosophila embryo (Abreu-Blanco et al., 2011). We did not observe injury-enriched labeling for a panel of additional dysferlin-interacting or muscular dystrophy proteins, or endomembrane or vesicle

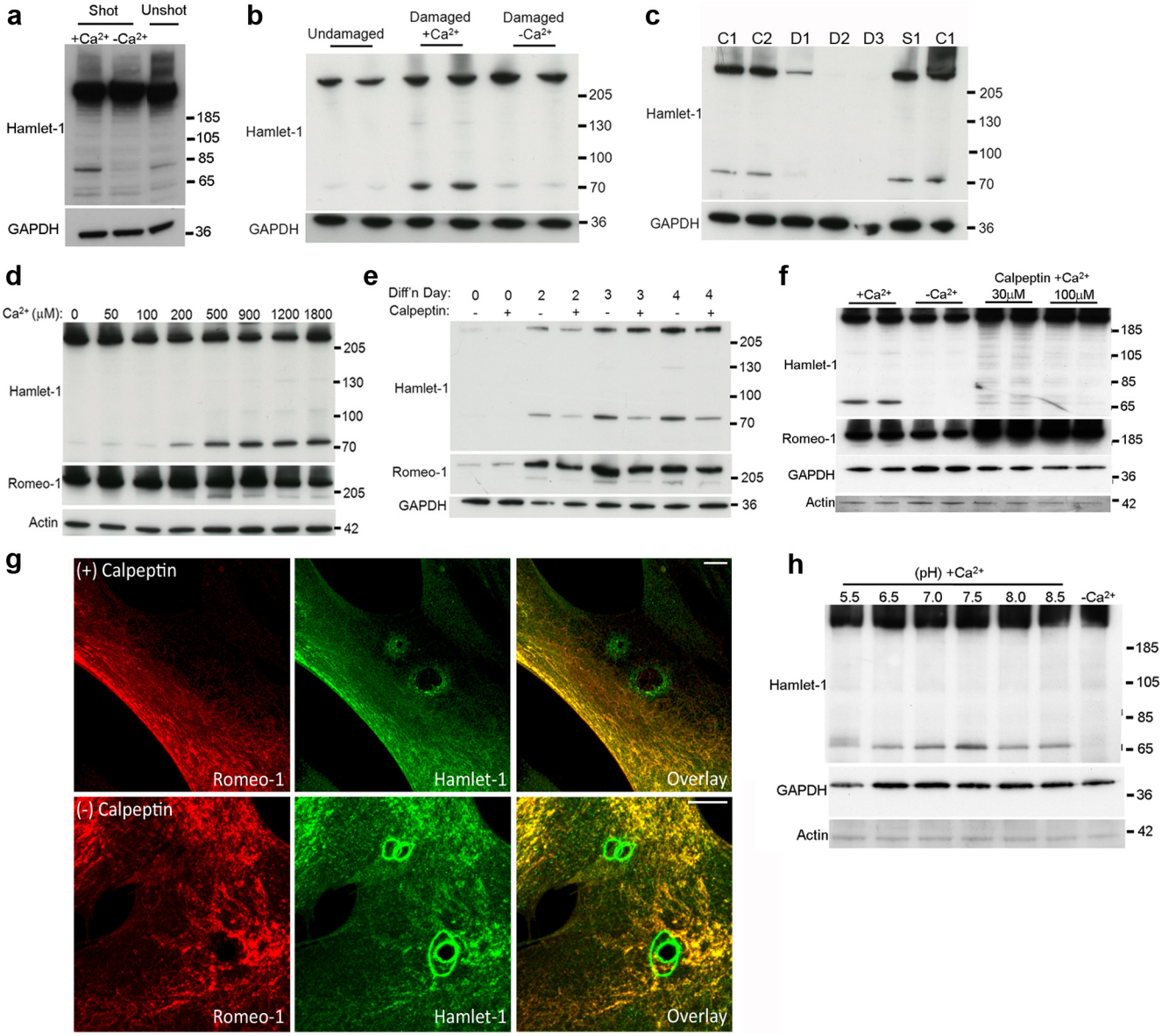

Figure 5. Membrane injury triggers calpain cleavage of dysferlin to release a C-terminal mini-dysferlin$_{C72}$ fragment with a specialized role in membrane repair. ***a***, A mini-dysferlin band of 72 kDa is detected by Hamlet-1 with ballistics injury in +Ca (lane 1), but not when injured in calcium-free buffer (lane 2) or in uninjured cells (lane 3). ***b***, Mini-dysferlin$_{C72}$ is also produced with scrape injury in +Ca (lanes 3 and 4), but not when injured in calcium-free buffer (lanes 5 and 6), or in uninjured cells (lanes 1 and 2). ***c***, Injury-induced production of mini-dysferlin$_{C72}$ is attenuated or absent in myotubes from three patients with dysferlinopathy (D1-D3) but normal in myotubes from disease controls (α-sarcoglycanopathy S1, caveolinopathy C1). ***d***, Production of mini-dysferlin$_{C72}$ is calcium-dependent, activated by 200 μM extracellular calcium. ***e***, Formation of mini-dysferlin$_{C72}$ is inhibited by calpeptin treatment. Differentiating myoblasts were treated with 20 μM calpeptin or DMSO carrier 24 and 3 h before harvesting. D0-D4, days of differentiation. ***f***, Maximal inhibition of dysferlin cleavage is achieved with $\geq$30 μM calpeptin using a 3 h preincubation treatment and refreshment of one-third media 30 min before injury. ***g***, Dysferlin recruitment to sites of ballistics injury is attenuated in calpeptin-treated myotubes (top row, Hamlet-1), compared with untreated human myotubes. ***h***, Maximum cleavage of dysferlin occurs at neutral pH. Cells were subjected to scrape injury in PBS buffered from pH 5.5–8.5.

markers (Fig. 3). In contrast to results by Reddy et al. (2001.) in fibroblasts, lysosomal markers were not enriched at sites of membrane injury in human myotubes, although we occasionally observed evidence for lysosomal exocytosis at sites distal to the membrane injury (Fig. 3).

A calpain-cleaved C-terminal fragment of dysferlin, mini-dysferlin$_{C72}$, has a specialized role in membrane repair

Our ballistics assay also revealed that dysferlin may be detected at sites of injury with antibodies recognizing a C-terminal epitope (Hamlet-1), but not N-terminal epitopes (i.e., Romeo, Hamlet-2, SAB2100636) (Fig. 4), raising the possibility of a truncated dysferlin isoform. We used Western analysis to look for a "mini-dysferlin" and observed a ~72 kDa C-terminal dysferlin isoform in myotubes shot in the presence of calcium but absent in myotubes shot without extracellular calcium and in unshot myotubes (Fig. 5*a*). To obtain greater quantities of protein for biochemical studies, we induced mechanical injury to the myotube plasma membrane by scraping cells from the tissue culture substratum with a rubber policeman, and similarly observed calcium-dependent formation of a ~72 kDa C-terminal dysferlin fragment with scrape injury (Fig. 5*b*), herein referred to as mini-dysferlin$_{C72}$. Injury-specific formation of mini-dysferlin$_{C72}$ was not observed in primary myotubes from three dysferlinopathy patients (Fig. 5*c*, D1–3), each possessing at least one allele with an intact 3′ region of their *DYSF* gene. These results negate the like-

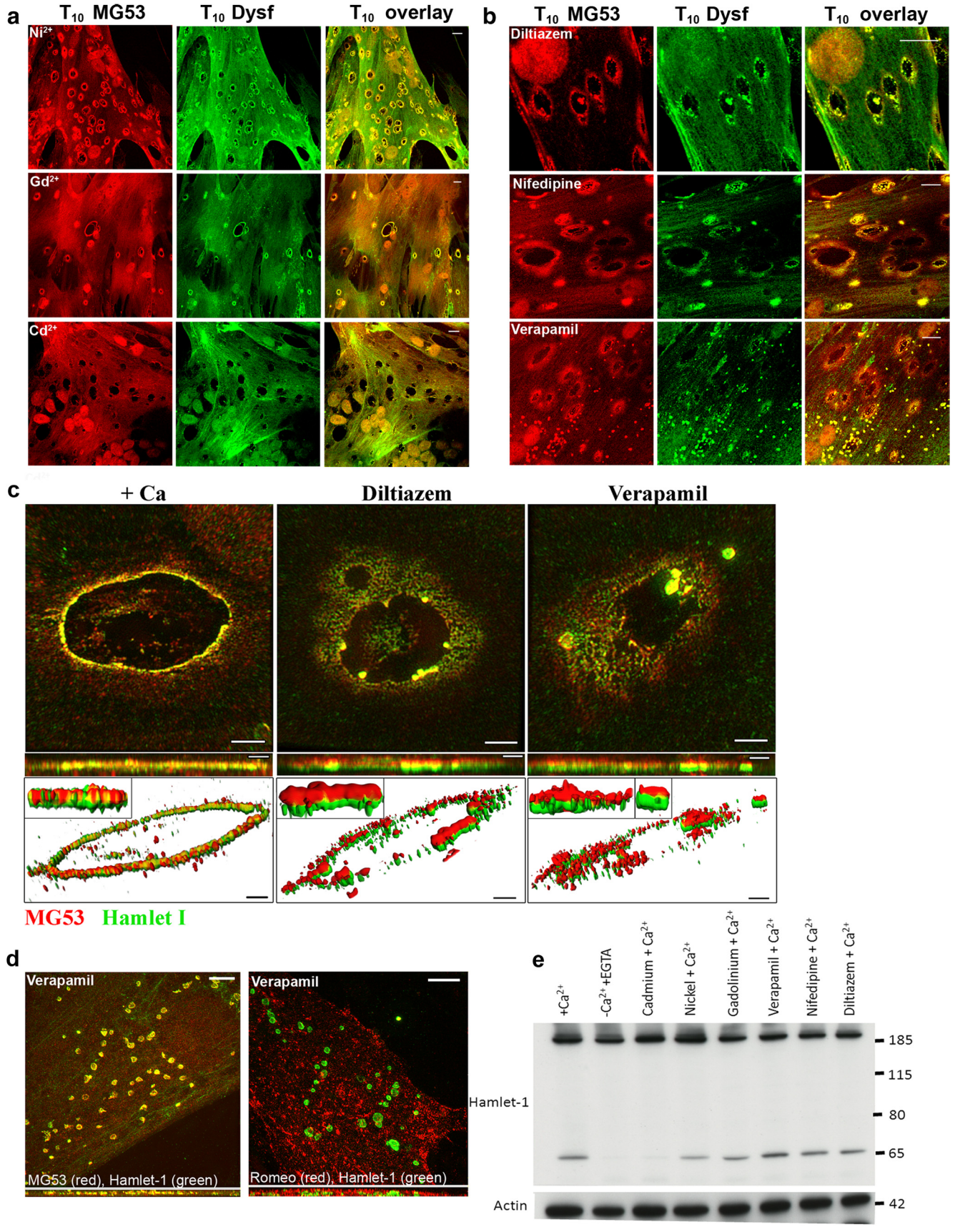

Figure 6. L-type calcium-channel signaling mediates coordinated fusion of mini-dysferlin$_{C72}$ rich cytoplasmic vesicles with MG53 plasma membrane domains. ***a***, Injury recruitment of dysferlin and MG53 is blocked by Cd^{2+}, but not by Ni^{2+} or Gd^{3+}. Scale bar, 10 μm. ***b***, Specific L-type channel antagonists diltiazem, nifedipine, and verapamil attenuate dysferlin and MG53 injury recruitment. Scale bar, 10 μm. ***c***, 3D-SIM of ballistics injuries performed in the presence or absence of specific L-type channel antagonists diltiazem and verapamil. Recruitment (*Figure legend continues.*)

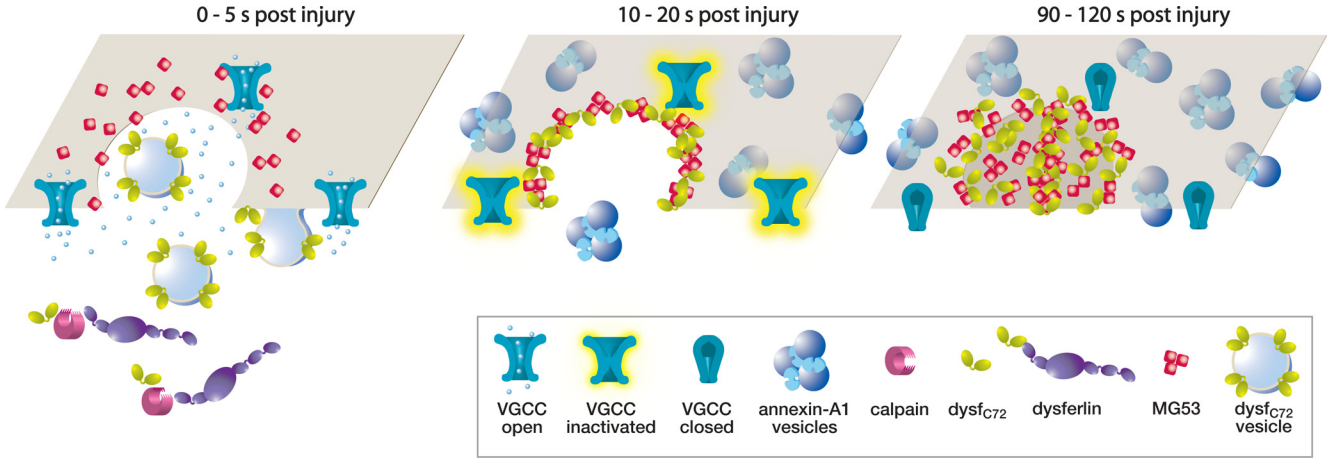

Figure 7. Our proposed model for membrane repair. 0–5 s after injury: Membrane injury causes promiscuous influx of calcium at sites of membrane injury, local activation of calpains, and strong and persistent depolarization of L-type VGCCs. MG53 is mobilized and targeted to the injury site. Injury mobilization of MG53 is calcium-independent and may relate to its role as a ubiquitin ligase, perhaps targeting a receptor damaged by oxidation or calpain cleavage as a consequence of the membrane injury. Dysferlin is cleaved by activated calpains, releasing a C-terminal fragment, mini-dysferlin$_{C72}$. Mini-dysferlin$_{C72}$-rich cytoplasmic vesicles are rapidly recruited to sites of membrane injury and fuse with MG53-decorated plasma membrane compartments in a calcium-dependent process coordinated by L-type VGCCs. 2–10 s after injury: Mini-dysferlin$_{C72}$ fuses into the plasma membrane and undergoes calcium-dependent phospholipid binding via its C2 domains, initiating a calcium-dependent phase of MG53 injury recruitment. Mini-dysferlin$_{C72}$ and MG53 compartments interact to form an interdigitated lattice with strong affinity for exposed phospholipids surrounding the injury site. 10–30 s after injury: Annexin-A1 undergoes calcium-activated phospholipid binding. The role of annexin-A1 may be related to delivery of endomembrane compartments peripheral to the injury site to reduce plasma membrane tension and facilitate repair. 30–120 s after injury: Mini-dysferlin$_{C72}$ and MG53 compartments infiltrate the plasma membrane surrounding the membrane injury, forming a lattice to stabilize the plasma membrane as it expands to reseal the membrane injury.

lihood of an alternate splice isoform and suggest mini-dysferlin$_{C72}$ is derived from full-length dysferlin.

Closely correlating with our ballistics immunostaining results, robust detection of mini-dysferlin$_{C72}$ by Western blot required an activating concentration of extracellular calcium ≥200 μM (Fig. 5*d*, Hamlet-1) and was accompanied by detection of the corresponding N-terminal ~170 kDa cleavage product (Fig. 5*d*, Romeo-1). With results showing injury-dependent and calcium-dependent dysferlin cleavage, we explored a role for calpains and showed that pretreatment of human skeletal myotubes with the calpain inhibitor calpeptin significantly attenuated formation of mini-dysferlin$_{C72}$ by Western blot with scrape injury (Fig. 5*e*) and reduced levels of recruited dysferlin in myotubes damaged by ballistics (Fig. 5*g*). The levels of cleaved mini-dysferlin$_{C72}$ relative to full-length dysferlin did not vary with myogenic differentiation, suggesting that capacity to cleave dysferlin in response to injury is not dependent upon the myogenic maturity of the sample (Fig. 5*e*). Through refinement of the calpeptin treatment regimen, we determined maximal inhibition of injury-activated dysferlin cleavage with ≥30 μM calpeptin using 3 h preincubation and refreshment of a third of the media 30 min before injury (Fig. 5*f*). To further support a role for calpains in the injury-specific cleavage of dysferlin, we performed scrape injury experiments in PBS buffered from pH 5.5–8.5, and demonstrated that maximum levels of cleaved mini-dysferlin$_{C72}$ occur at neutral pH 7.5 (Fig. 5*h*).

Collectively, our results indicate that dysferlin is a substrate of activated calpains, releasing a C-terminal fragment with a specific role in membrane repair. Molecular weight calculations predict that mini-dysferlin$_{C72}$ includes the two most ancestrally conserved C2 domains (Lek et al., 2010), with structural parallels to the classical mediators of vesicle fusion, the synaptotagmins.

Injury-recruitment of dysferlin and MG53 is blocked by cadmium and attenuated by L-type voltage-gated channel antagonists

Given that otoferlin (Ramakrishnan et al., 2009) and sea-urchin ferlin (Covian-Nares et al., 2010) are regulated by specific VGCCs, we explored a role for VGCC in the regulation of dysferlin in membrane repair. First, we used broad nonspecific blockers of different classes of VGCC and showed cadmium (Cd; blocks L-, P-, and R-types), but not nickel (Ni; blocks P/Q-, R-, and T-types) or gadolinium (Gd; blocks stretch-activated channels), blocked recruitment of MG53 and dysferlin to sites of membrane injury, and detection of mini-dysferlin$_{C72}$ by Western blot (Fig. 6*a*). Cadmium is a classical inhibitor of L-type channels, although it may exert off-target effects with access to the cellular cytoplasm after membrane injury. Therefore, we examined the effects of specific L-type channel antagonists and showed that diltiazem, nifedipine, and verapamil blocked or attenuated injury-induced recruitment of dysferlin and MG53 (Fig. 6*b*). None of the specific L-type antagonists blocked formation of cleaved mini-dysferlin$_{C72}$ detected by Western blot (Fig. 6*e*); rather, they appeared to induce an uncoordinated vesicle fusion response, with "clumps" of mini-dysferlin$_{C72}$ and MG53 at the lesion circumference (Fig. 6*b*,*c*). Super-resolution 3D-SIM shows distinct spatial separation of the dysferlin and MG53 in the presence of L-type VGCC antagonists, with dysferlin (green) lying on the cytoplasmic face of MG53 (red) membrane compartments (Fig. 6*c*), similar to low-calcium conditions (Fig. 1*a*). In

←

(*Figure legend continued.*) of dysferlin and MG53 is attenuated and appears uncoordinated, with clumps of dysferlin and MG53 at the edges of the lesions (*xy*, scale bar, 2 μm, MG53 red, Hamlet-1 green). Rotation of images in the *xz* or *yz* planes (scale bars, 1 μm) reveals spatial separation of dysferlin and MG53 compartments, similar to low calcium conditions (Fig. 1). ***d***, 3D-SIM of large vesicles generated by verapamil treatment. The diameter of vesicles was 0.82 ± 0.4 μm (mean ± SD); $n = 222$. Vesicles positively label for MG53 and the C-terminal dysferlin antibody Hamlet-1 (left), but not the N-terminal dysferlin antibody Romeo-1, suggesting that they represent abnormal fusion of mini-dysferlin$_{C72}$ and MG53 compartments. Romeo separately labels a population of smaller vesicles that are negative for Hamlet-1, suggesting separate subcellular localizations for each of the cleaved dysferlin fragments. ***e***, Cadmium inhibits formation of mini-dysferlin$_{C72}$ detected by Western blot, with normal production of mini-dysferlin$_{C72}$ observed with Ni^{2+}, Gd^{3+}, and specific L-type VGCC antagonists.

the case of verapamil treatment, we also observed formation of a population of abnormally large vesicles containing cleaved mini-dysferlin$_{C72}$ and MG53 (i.e., positive for C-terminal Hamlet-1, but negative for N-terminal Romeo-1) (mean diameter 0.8 μm, range 0.3–3.7 μm; Fig. 6*d*). Our results suggest that, despite promiscuous calcium entry through wound sites, VGCCs play a role in coordinating the regulated fusion of mini-dysferlin$_{C72}$ and MG53 compartments for membrane repair.

Discussion

Collectively, our results implicate two cooperative calcium signaling cascades for muscle membrane repair, separately activated by calcium entry through membrane lesions, as well as specific calcium signaling via L-type VGCC. We refine the muscle membrane repair paradigm to propose the following working model (Fig. 7). Membrane injury causes promiscuous influx of calcium at sites of membrane injury, local activation of calpains, and strong and persistent depolarization of L-type VGCC. Dysferlin is cleaved by activated calpains, releasing a C-terminal fragment, mini-dysferlin$_{C72}$. Mini-dysferlin$_{C72}$-rich cytoplasmic vesicles are rapidly recruited to sites of membrane injury and fuse with MG53 decorated plasma membrane compartments in a process coordinated by L-type VGCC. Mini-dysferlin$_{C72}$ undergoes calcium-dependent protein or phospholipid binding via its C2 domains, initiating a calcium-dependent phase of MG53 injury recruitment. The role of MG53 at sites of membrane injury may relate to its functions as a phosphatidylserine binding protein and a ubiquitin ligase; MG53 may be initially recruited via calcium-independent mechanisms to rapidly ubiquitinate target receptors/channels (currently unknown) damaged by the membrane injury to target them for recycling/repair or degradation.

3D-SIM provides the first evidence that mini-dysferlin$_{C72}$ is delivered to sites of membrane injury in cytoplasmic vesicles that align and fuse with plasma membrane domains enriched with MG53 in a process coordinated by L-type VGCCs, a role consistent with VGCC-regulated vesicle fusion of mammalian otoferlin (Ramakrishnan et al., 2009) and sea-urchin ferlin (Covian-Nares et al., 2010). Interestingly, a role for L-type channels in response to acute membrane injury of transected spinal cord axons has been reported (Nehrt et al., 2007), suggesting that L-type channels may mediate cellular signaling in response to acute membrane injuries in other tissues.

Annexin-A1 did not specifically label injury sites, and showed different temporal activation and biodistribution in injured myotubes, suggesting that annexin-A1 may participate in a separate arm of the membrane repair response. Repaired lesions were often characterized by a dominant arc of mini-dysferlin$_{C72}$ and MG53 among an interdigitated lattice. This pattern of labeling is consistent with a repair model whereby mini-dysferlin$_{C72}$ and MG53 initially bind the exposed edge of the damage site, then infiltrate and stabilize the surrounding bilayer as it expands to reseal the membrane injury. The membrane arc represents the edges of the original lesion that are elongated, aligned, and pushed centrally as new membrane is added to the lesion surrounds to facilitate resealing of the membrane breach.

A specific role for mini-dysferlin$_{C72}$ in membrane repair is consistent with studies described by Roostalu and Strahle (2012), who developed an elegant *in vivo* model of muscle membrane damage in a developing zebrafish embryo and showed that C-terminal fragments of ectopically expressed human dysferlin showed injury recruitment, but N-terminal fragments did not. Furthermore, biologically derived mini-dysferlin$_{C72}$ bears similarity to a truncated dysferlin identified in a mildly affected dysferlinopathy patient with a genomic deletion within the *DYSF* gene (Krahn et al., 2010). Remarkably, this patient-derived mini-dysferlin also bears the last two C2 domains and transmembrane domain and was shown to functionally restore defective membrane repair when expressed in dysferlin-deficient mouse muscle fibers (Krahn et al., 2010).

Our discovery that activated calpains generate mini-dysferlin$_{C72}$ with a specialized role in membrane repair reveals a novel function for calpains in the cellular response to membrane injury and is consistent with studies by Mellgren et al. (2009) that establish a requirement for m- or μ-calpain, but not calpain-3, for muscle membrane repair. m-Calpain and μ-calpain are named based on their activating calcium concentrations in the millimolar or micromolar range, respectively (Cong et al., 1989; Goll et al., 2003). In our study, 200 μM extracellular calcium was the critical concentration required for both biochemical detection of cleaved mini-dysferlin$_{C72}$ (Fig. 5) and for tight refinement of dysferlin and MG53 into concentrated rings encircling sites of membrane injury by immunolabeling (Fig. 1). However, this calcium concentration does not clearly implicate one calpain over another and may also reflect a critical extracellular calcium concentration for conductance and signaling by L-type calcium channels to recruit or activate vesicle fusion.

Analysis of the biodistribution (Murphy et al., 2006), autolysis (Murphy et al., 2006), and damage-induced activity (Gailly et al., 2007) of calpains in single muscle fibers reveals a population of membrane-associated preactivated μ-calpain previously proposed as ideally positioned to rapidly mediate a role in membrane resealing (for review, see Lamb, 2007). In −Ca conditions, a cleaved mini-dysferlin$_{C72}$ (positive for Hamlet-1 but negative for the N-terminal Romeo-1 epitope) shows a diffuse halo of enrichment within 10 seconds of a membrane injury. However, it is important to consider that ballistics will also structurally damage intracellular calcium stores and induce local elevations in intracellular calcium that may be sufficient for calpain activation. Further studies are required to define roles of μ-calpain and m-calpain in dysferlin cleavage and membrane repair, to refine feasible scenarios that include potential roles for both isoforms; for example, preactivated μ-calpain may cleave dysferlin, whereas activated m-calpain may remodel the cytoskeleton associated with the expansion and contraction stages of membrane repair (Fig. 2) (Abreu-Blanco et al., 2011).

Collectively, our results confirm that muscle cells use a mechanism similar to synaptic exocytosis for membrane repair (Steinhardt et al., 1994). The structural similarity between synaptotagmins and the predicted structure of cleaved mini-dysferlin$_{C72}$ cannot be overlooked, and suggests functional parallels between protein- or phospholipid-binding roles of mini-dysferlin$_{C72}$ in membrane repair and that of synaptotagmin for secretory exocytosis. Importantly, our results suggest that cellular functions of dysferlin, and perhaps other mammalian ferlins, may be diversified via enzymatic cleavage to release different C2 domain-containing fragments with specialized functions. Our results shed new light on the established paradigm of calcium-dependent membrane repair, highly relevant to disease pathogenesis in dysferlinopathy, and perhaps also relevant to other pathologies characterized by calcium signaling with membrane injury.

References

Abreu-Blanco MT, Verboon JM, Parkhurst SM (2011) Cell wound repair in Drosophila occurs through three distinct phases of membrane and cytoskeletal remodeling. J Cell Biol 193:455–464. CrossRef Medline

Bansal D, Miyake K, Vogel SS, Groh S, Chen CC, Williamson R, McNeil PL,

Campbell KP (2003) Defective membrane repair in dysferlin-deficient muscular dystrophy. Nature 423:168–172. CrossRef Medline

Bashir R, Britton S, Strachan T, Keers S, Vafiadaki E, Lako M, Richard I, Marchand S, Bourg N, Argov Z, Sadeh M, Mahjneh I, Marconi G, Passos-Bueno MR, Moreira Ede S, Zatz M, Beckmann JS, Bushby K (1998) A gene related to Caenorhabditis elegans spermatogenesis factor fer-1 is mutated in limb-girdle muscular dystrophy type 2B. Nat Genet 20:37–42. CrossRef Medline

Bouter A, Gounou C, Berat R, Tan S, Gallois B, Granier T, d'Estaintot BL, Poschl E, Brachvogel B, Brisson AR (2011) Annexin-A5 assembled into two-dimensional arrays promotes cell membrane repair. Nat Commun 2:272. CrossRef Medline

Cai C, Masumiya H, Weisleder N, Matsuda N, Nishi M, Hwang M, Ko JK, Lin P, Thornton A, Zhao X, Pan Z, Komazaki S, Brotto M, Takeshima H, Ma J (2009a) MG53 nucleates assembly of cell membrane repair machinery. Nat Cell Biol 11:56–64. CrossRef Medline

Cai C, Weisleder N, Ko JK, Komazaki S, Sunada Y, Nishi M, Takeshima H, Ma J (2009b) Membrane repair defects in muscular dystrophy are linked to altered interaction between MG53, caveolin-3, and dysferlin. J Biol Chem 284:15894–15902. CrossRef Medline

Cong J, Goll DE, Peterson AM, Kapprell HP (1989) The role of autolysis in activity of the Ca^{2+}-dependent proteinases (mu-calpain and m-calpain). J Biol Chem 264:10096–10103. Medline

Costes SV, Daelemans D, Cho EH, Dobbin Z, Pavlakis G, Lockett S (2004) Automatic and quantitative measurement of protein-protein colocalization in live cells. Biophys J 86:3993–4003. CrossRef Medline

Covian-Nares JF, Koushik SV, Puhl HL 3rd, Vogel SS 2010 Membrane wounding triggers ATP release and dysferlin-mediated intercellular calcium signaling. J Cell Sci 123:1884–1893. Medline

Dulon D, Safieddine S, Jones SM, Petit C (2009) Otoferlin is critical for a highly sensitive and linear calcium-dependent exocytosis at vestibular hair cell ribbon synapses. J Neurosci 29:10474–10487. CrossRef Medline

Gailly P, De Backer F, Van Schoor M, Gillis JM (2007) In situ measurements of calpain activity in isolated muscle fibres from normal and dystrophin-lacking mdx mice. J Physiol 582:1261–1275. CrossRef Medline

Goll DE, Thompson VF, Li H, Wei W, Cong J (2003) The calpain system. Physiol Rev 83:731–801. CrossRef Medline

Gustafsson MG, Shao L, Carlton PM, Wang CJ, Golubovskaya IN, Cande WZ, Agard DA, Sedat JW (2008) Three-dimensional resolution doubling in wide-field fluorescence microscopy by structured illumination. Biophys J 94:4957–4970. CrossRef Medline

Johnson CP, Chapman ER (2010) Otoferlin is a calcium sensor that directly regulates SNARE-mediated membrane fusion. J Cell Biol 191:187–197. CrossRef Medline

Krahn M, Wein N, Bartoli M, Lostal W, Courrier S, Bourg-Alibert N, Nguyen K, Vial C, Streichenberger N, Labelle V, DePetris D, Pécheux C, Leturcq F, Cau P, Richard I, Lévy N (2010) A naturally occurring human minidysferlin protein repairs sarcolemmal lesions in a mouse model of dysferlinopathy. Sci Transl Med 2:50ra69. Medline

Lamb GD (2007) Calpains in muscle: selective and protective? J Physiol 582:897. CrossRef Medline

Lek A, Lek M, North KN, Cooper ST (2010) Phylogenetic analysis of ferlin genes reveals ancient eukaryotic origins. BMC Evol Biol 10:231. CrossRef Medline

Lek A, Evesson FJ, Sutton RB, North KN, Cooper ST (2012) Ferlins: regulators of vesicle fusion for auditory neurotransmission, receptor trafficking and membrane repair. Traffic 13:185–194. CrossRef Medline

Liu J, Aoki M, Illa I, Wu C, Fardeau M, Angelini C, Serrano C, Urtizberea JA, Hentati F, Hamida MB, Bohlega S, Culper EJ, Amato AA, Bossie K, Oeltjen J, Bejaoui K, McKenna-Yasek D, Hosler BA, Schurr E, Arahata K, de Jong PJ, Brown RH Jr (1998) Dysferlin, a novel skeletal muscle gene, is mutated in Miyoshi myopathy and limb girdle muscular dystrophy. Nat Genet 20:31–36. Medline

McNeil AK, Rescher U, Gerke V, McNeil PL (2006) Requirement for annexin A1 in plasma membrane repair. J Biol Chem 281:35202–35207. CrossRef Medline

Mellgren RL, Miyake K, Kramerova I, Spencer MJ, Bourg N, Bartoli M, Richard I, Greer PA, McNeil PL (2009) Calcium-dependent plasma membrane repair requires m- or mu-calpain, but not calpain-3, the proteasome, or caspases. Biochim Biophys Acta 1793:1886–1893. CrossRef Medline

Murphy RM, Verburg E, Lamb GD (2006) Ca2+ activation of diffusible and bound pools of mu-calpain in rat skeletal muscle. J Physiol 576:595–612. CrossRef Medline

Nehrt A, Rodgers R, Shapiro S, Borgens R, Shi R (2007) The critical role of voltage-dependent calcium channel in axonal repair following mechanical trauma. Neuroscience 146:1504–1512. CrossRef Medline

Ramakrishnan NA, Drescher MJ, Drescher DG (2009) Direct interaction of otoferlin with syntaxin 1A, SNAP-25, and the L-type voltage-gated calcium channel Cav1.3. J Biol Chem 284:1364–1372. CrossRef Medline

Reddy A, Caler EV, Andrews NW (2001) Plasma membrane repair is mediated by Ca(2+)-regulated exocytosis of lysosomes. Cell 106:157–169. CrossRef Medline

Riglar DT, Richard D, Wilson DW, Boyle MJ, Dekiwadia C, Turnbull L, Angrisano F, Marapana DS, Rogers KL, Whitchurch CB, Beeson JG, Cowman AF, Ralph SA, Baum J (2011) Super-resolution dissection of coordinated events during malaria parasite invasion of the human erythrocyte. Cell Host Microbe 9:9–20. CrossRef Medline

Roostalu U, Strähle U (2012) In vivo imaging of molecular interactions at damaged sarcolemma. Dev Cell 22:515–529. CrossRef Medline

Roux I, Safieddine S, Nouvian R, Grati M, Simmler MC, Bahloul A, Perfettini I, Le Gall M, Rostaing P, Hamard G, Triller A, Avan P, Moser T, Petit C (2006) Otoferlin, defective in a human deafness form, is essential for exocytosis at the auditory ribbon synapse. Cell 127:277–289. CrossRef Medline

Schermelleh L, Carlton PM, Haase S, Shao L, Winoto L, Kner P, Burke B, Cardoso MC, Agard DA, Gustafsson MG, Leonhardt H, Sedat JW (2008) Subdiffraction multicolor imaging of the nuclear periphery with 3D structured illumination microscopy. Science 320:1332–1336. CrossRef Medline

Steinhardt RA, Bi G, Alderton JM (1994) Cell membrane resealing by a vesicular mechanism similar to neurotransmitter release. Science 263:390–393. CrossRef Medline

Waddell LB, Lemckert FA, Zheng XF, Tran J, Evesson FJ, Hawkes JM, Lek A, Street NE, Lin P, Clarke NF, Landstrom AP, Ackerman MJ, Weisleder N, Ma J, North KN, Cooper ST (2011) Dysferlin, annexin A1, and mitsugumin 53 are upregulated in muscular dystrophy and localize to longitudinal tubules of the T-system with stretch. J Neuropathol Exp Neurol 72:302–313. CrossRef Medline

Washington NL, Ward S (2006) FER-1 regulates Ca2+-mediated membrane fusion during C. elegans spermatogenesis. J Cell Sci 119:2552–2562. CrossRef Medline